

AN EXPERIMENTAL AND ANALYTICAL INVESTIGATION OF A TURBULENT AXISYMMETRIC JET IN A VISCOUS HOST FLUID

Léa Voivenel
CORIA UMR 6614
University of Rouen
76801 Saint Etienne du Rouvray FRANCE

Luminita Danaila
CORIA UMR 6614
University of Rouen
76801 Saint Etienne du Rouvray FRANCE

Emilien Varea
CORIA UMR 6614
University of Rouen
76801 Saint Etienne du Rouvray FRANCE

Bruno Renou
CORIA UMR 6614
University of Rouen
76801 Saint Etienne du Rouvray FRANCE

Michel Cazalens
SAFRAN Research and Technologies Centre
78772 Magny-les-Hameaux FRANCE

ABSTRACT

Turbulent jets have received considerable attention during the last decades and the past century. However, to our knowledge, one configuration has not received much consideration yet. The latter concerns the viscosity-stratified jet, wherein a turbulent jet of lower viscosity issues into a density-matched host fluid of higher viscosity. In this paper, we shed more light over some intricacies of viscosity-stratified flows, by addressing two issues:

i) **Experimental aspect.** A propane jet issues into a N_2 (slight) coflow, for which the viscosity ratio is $R_v \equiv \nu_{N_2} / \nu_{propane} = 3.5$. The Reynolds number of the jet (based on the diameter, the initial velocity and the propane viscosity), is of 8000. Experimental results are discussed, for both velocity and scalar fields, in the axial plane of the turbulent axisymmetric jet. It is shown that the presence of a strong viscosity discontinuity across the jet edge results in an increase of the scalar spread rate and of the turbulent fluctuations.

ii) **Analytical developments and consequences.** One- and two-point energy budget equations are developed for flows in which the viscosity varies, as a result of heterogeneous mixture. Additional terms are highlighted, accounting for mean viscosity gradients or correlations between viscosity fluctuations and kinetic energy fluctuations. These terms are most likely present at both small and large scales, thus rectifying the myth that viscosity is a small-scale quantity. It is finally shown that, unlike the classical round jet issuing into a host fluid with the same viscosity, the condition of self-preservation on the jet axis is not necessarily satisfied in variable-viscosity jets.

INTRODUCTION

The theory of Kolmogorov premises that at infinitely large Reynolds numbers, the statistical properties of the small scales should be determined universally by ν and $\bar{\epsilon}$ (the kinematic viscosity and the mean energy dissipation rate). Implicit to this theory is that viscosity, considered as one independent parameter of the flow, is a 'small scale' quantity and thus should not affect large scale mixing. This is one possible explanation for why most of the studies focus on variable-density flows (Pitts (1991), Amielh *et al.* (1996)). Nonetheless, many flows deal with real fluids, for which both density and viscosity fluctuate in space and time.

One of the first studies devoted to effects of viscosity was that of Campbell & Turner (1986). In order to determine the composition of a magmatic layer, they studied the injection of a fluid in a more viscous one (whose kinematic viscosities are respectively ν_l and ν_h , indices 'l' and 'h' stand for 'low' and 'high' respectively), for several ratios $R_v = \frac{\nu_h}{\nu_l}$ spread from 1 to 400. Campbell & Turner (1986) observed a very different behaviour for the two borderline-cases. Indeed, mixing does not occur at all for the $R_v = 400$ case. This phenomenon is due to a competition between the destabilizing inertial forces and the stabilizing viscous ones at the interface. Thus, this study highlights that the large scale mixing is in fact, greatly, viscosity-dependant and that Variable-Viscosity-Flow (hereafter referred to as VVF) should be carefully studied. Indeed, this kind of flow is frequently encountered in industrial applications. To cite one example, combustion processes involve fluids with different physical and chemical properties (*e.g.* fuel and oxidizer).

Numerous questions, however, remain without clear

answer. Some of them are fundamental, such as those dealing with the rate of entrainment and the associated phenomenology, or the exact expression of the mean energy dissipation rate (Talbot *et al.* (2013), Lee *et al.* (2008)) which appears to be of great importance for flame stabilization and quenching. Hence, it is necessary to perform some quantitative experiments in more traditional aerodynamic configurations (gaseous flow and relatively high Reynolds number).

The present study aims at furthering our understanding of variable-viscosity flows. The roadmap of the paper is as follows. The first section details the experimental facility and results on the dynamic and scalar fields. Then, the two-point scale-by-scale energy budgets are developed by considering viscosity variations within the flow. The third section aims at answering the question of similarity in VVF. The last part is dedicated to conclusions.

EXPERIMENTAL STUDY

Experimental set-up. The flow facility in which the following results are obtained is a round jet of $D = 30$ mm diameter surrounded by a (slight) coflow. Jet and coflow are enclosed in order to get well defined boundary conditions allowing future accurate numerical simulations (Fig.1). The

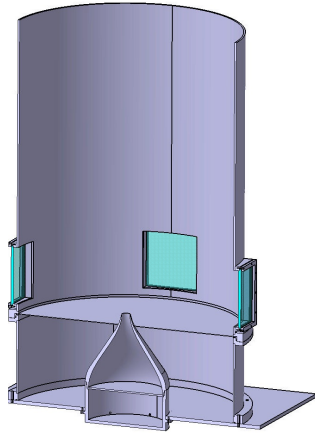


Figure 1. Experimental facility.

main jet issues from a contraction designed to ensure a 'top-hat' velocity profile at the nozzle exit. The initial turbulence intensity is as low as 1%, thus ensuring that the measured turbulent fluctuations do not find their origins in the injection.

The viscous effects are quantified by comparing the following cases:

- Constant-Viscosity Flow (CVF), which is the baseline case. A nitrogen jet issues in a coflow of nitrogen. The viscosity ratio of the two fluids is $R_v = 1$.

- Variable-Viscosity Flow (VVF). A propane jet issues in a coflow of nitrogen. The latter is 3.5 times more viscous than the propane, so that $R_v = 3.5$. The density ratio is very nearly equal to 1. The comparison between the two cases is based on the *same initial condition*, i.e. the same initial jet momentum, therefore the same injection velocity $U_1 = 1.45$ m/s.

Measurements were performed in both configurations for the 2-D velocity fields (by stereo-Particle Image Ve-

locimetry PIV) and for the scalar (by PLIF Planar Laser Induced Fluorescence). The seeding for PLIF was done by anisole for both configurations. Indeed, the lack of oxygen allows us to use an aromatic tracer instead of classical ketone one, which leads to an improved signal-to-noise ratio.

Results. Figure 2 illustrates instantaneous images of the scalar distribution. Here Y is the propane concentration, (or, the mixture fraction), normalized such as $Y = 1$ in the propane core jet and $Y = 0$ in the N_2 coflow. A careful analysis of the scalar mixing provides a qualitative way to compare the two flows. Whilst the constant-viscosity flow exhibits classical Kelvin-Helmholtz vortices (Fig. 2, top), the variable-viscosity flow (Fig. 2, bottom) only includes a hint of the large-scale, lateral engulfment of the ambient fluid, living together with mixing at scales distributed over a much wider range.

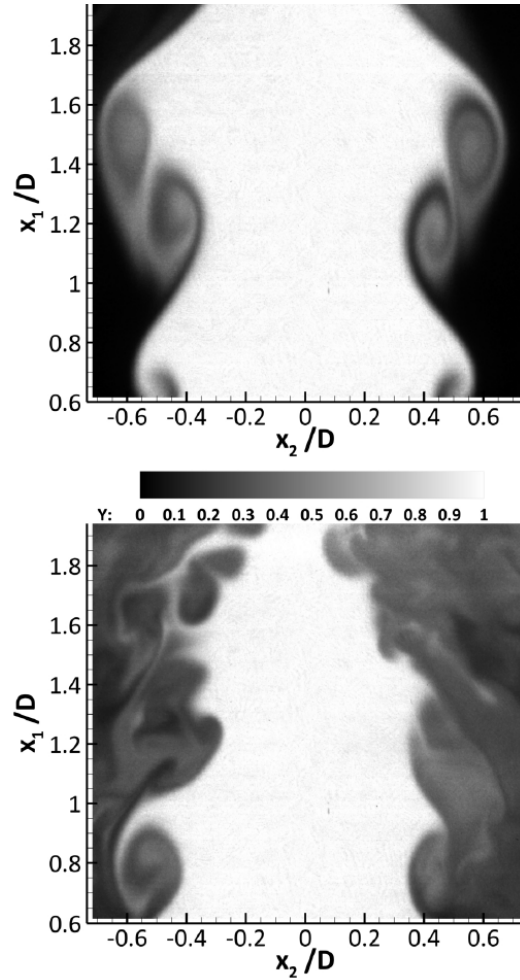


Figure 2. Instantaneous images of mixing in N_2/N_2 jet (top) and variable-viscosity (propane/ N_2) jet (bottom).

Planar distributions of the RMS (root mean squared) of the scalar are represented in Fig. 3, for the very near field of the flow, spanning between the 0 and 2 jet diameters. Several observations may be done. First, the CVF potential core is wider than that of the VVF, which suggests a better mixing for the latter (Fig. 3, right-side). This statement is corroborated by the presence of propane in the full

field of view for VVF. This is in contrast with the N_2/N_2 jet, where the core jet fluid (seeded N_2) is completely absent on the image edges. Second, the largest RMS values are not located at the same axial locations: for the CVF flow, the largest values of the scalar RMS are located at $2D$, whereas for the VVF, these maxima occur at much smaller downstream locations ($0.5D - 1D$). This observation is to be understood in connection with the instantaneous images. The intense fluctuations are strongly correlated with the presence of the large structure (Kelvin Helmholtz). For the VVF case, while at $x/D = 1$ engulfment only occurs, the mixing exhibits smaller and smaller scales at $x/D = 2$. As far as

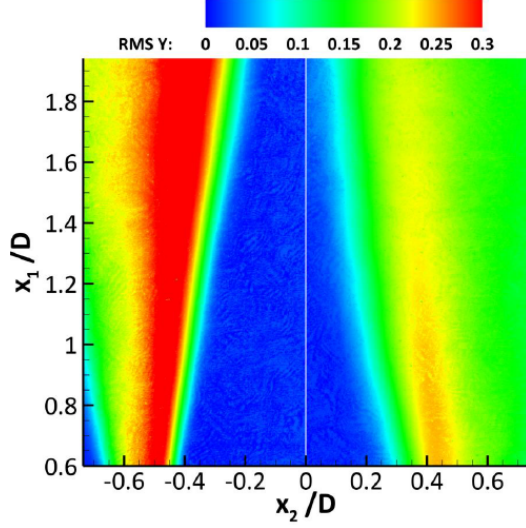


Figure 3. Planar distributions of the scalar RMS in CVF (N_2/N_2 jet), image left-side, and VVF (Propane/ N_2 jet), image right-side.

the CVF is concerned, only large-scale mixing occurs, thus explaining that larger fluctuations are observed.

This observation is strengthened by the study of the velocity field and more particularly of the mean lateral fluctuations (not shown here), whose evolution is similar to that of the scalar. Indeed, at a downstream position of one diameter, the lateral fluctuations are more intense in VVF than in CVF.

Moreover, a stronger decrease of the axial mean velocity in VVF than in CVF is also noticeable, starting in the very early stage of injection (Fig. 4), indicating an increased entrainment of the ambient fluid into the jet fluid and an accelerated trend towards self-similarity. Intense values of the axial velocity fluctuations (Fig. 5) as well as a faster trend towards isotropy (here quantified through the ratio RMS_{u_1}/RMS_{u_2} Fig. 6) in VVF than in the baseline case (CVF) are observed. These results confirm the trends previously reported by Talbot *et al.* (2013), along with the value of 1.2 for the RMS_{u_1}/RMS_{u_2} ratio Talbot (2009).

It is interesting to note that, independently of the quantity used for the comparison between the two flows, the discrepancies are more and more enhanced with increasing downstream locations. The birth of the turbulent fluctuations most likely results from a combination of four factors: *i*) Kelvin Helmholtz instabilities; *ii*) wake instabilities behind the injector lip; *iii*) interface instabilities due to density

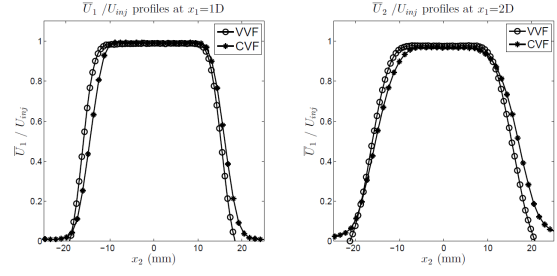


Figure 4. Mean axial velocity normalized with respect to the injection velocity, for both CVF and VVF, at two axial locations: $1D$ and $2D$.

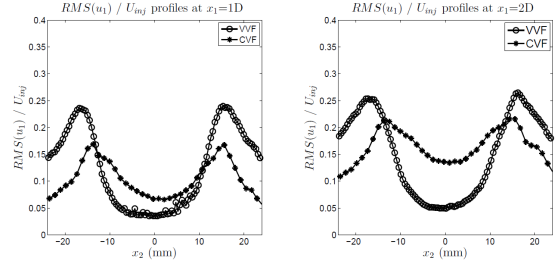


Figure 5. Radial RMS normalized with respect to the injection velocity, for both CVF and VVF, at two axial locations: $1D$ and $2D$.

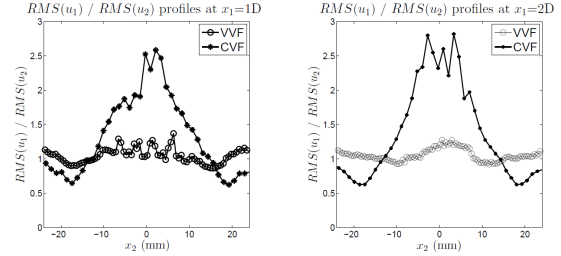


Figure 6. Ratio RMS_{u_1}/RMS_{u_2} for VVF and CVF, at two axial locations: $1D$ and $2D$.

gradients; *iv*) interface instabilities due to viscosity jumps. Points *i*) and *ii*) are characteristic of jet flows, constant-viscosity or not, thus, they can't be responsible for such different behaviors. As far as the density effects are concerned, the studied configuration is those of a 'heavy jet' (heavy fluid injected in a lighter one). Yet, according to (Amielh *et al.*, 1996), in this situation if the density effects prevailed they would inhibit the mixing and not enhance it as observed here. A phenomenological scenario to explain the mixing enhancement, based on point *iv*), is as follows. Viscous host fluid blobs are brought (via the three types of instabilities) into the jet fluid. These viscous blobs represent obstacles which slow down the initial jet velocity and lead to the production of radial velocity fluctuations behind these obstacles (wake instabilities). The rapid birth of radial velocity fluctuations accelerates the trend towards isotropy and self-similarity.

We conclude this section with the statement that clear experimental evidence has been brought to claim that viscosity stratification has an important influence on turbulence, for viscosity ratios as low as 3.5. In the following,

we develop the analytical tool aimed at deepening the investigation of VVF.

ANALYTICAL DEVELOPMENT

A deeper insight into the birth, increase and dissipation of turbulent fluctuations is provided by the one-point kinetic energy budget in variable-viscosity flows, Talbot *et al.* (2013). With the decomposition $U_i = \bar{U}_i + u_i$, the one-point kinetic energy budget is as follows:

$$\begin{aligned}
& \underbrace{\frac{\partial}{\partial t} (\overline{u_i^2})}_{NS} + \underbrace{\bar{U}_j \frac{\partial}{\partial x_j} (\overline{u_i^2})}_A + \underbrace{u_j \frac{\partial}{\partial x_j} (\overline{u_i^2})}_B \\
& + 2 \underbrace{\overline{u_i u_j} \frac{\partial \bar{U}_i}{\partial x_j}}_C = -2 \underbrace{\frac{\partial}{\partial x_i} \overline{u_i P}}_D \\
& + \underbrace{2 \overline{u_i \cdot v} \frac{\partial^2 \bar{U}_i}{\partial x_j^2} + v \frac{\partial^2 \overline{u_i^2}}{\partial x_j^2}}_E \\
& + 2 \underbrace{\frac{\partial v}{\partial x_j} \overline{u_i} \cdot \left[\frac{\partial \bar{U}_i}{\partial x_j} + \frac{\partial \bar{U}_j}{\partial x_i} \right]}_{P_{VG}} \\
& + \underbrace{\frac{\partial v}{\partial x_j} \frac{\partial \overline{u_i^2}}{\partial x_j} + 2 \frac{\partial v}{\partial x_j} \frac{\partial (\overline{u_i u_j})}{\partial x_i}}_{\mathcal{D}_{VG}} - 2v \underbrace{\left(\frac{\partial \overline{u_i}}{\partial x_j} \right)^2}_{\bar{\epsilon}_{VV}}. \quad (1)
\end{aligned}$$

Summation convention applies to repeated indices and overbar signifies time averaging. Term *NS* reflects the non-stationarity of the kinetic energy. Terms *A*, *B*, *C*, *D* and *E* represent respectively the kinetic energy advection, turbulent diffusion, production, pressure diffusion (the kinematic pressure is considered) and the molecular effects. An analysis of this equation has been performed for the particular case of a temporal mixing layer involving two streams with different viscosities, e.g. Taguelmimt *et al.* (2014). Terms \bar{P}_{VG} ('VG' stands for 'Viscosity Gradients') involve mean velocity gradients multiplied by correlations between viscosity gradients and velocity fluctuations. These are positive and contribute to the increase of the kinetic energy. Therefore, they are called 'Production due to Viscosity Gradients' (P_{VG}). Terms \mathcal{D}_{VG} reflect an overall destruction of fluctuations (although, the second term may become locally positive, Taguelmimt *et al.* (2014)). The last term represents the homogeneous form of $\bar{\epsilon}_{VV}$. This budget involves a complete expression of the mean energy dissipation rate, $\bar{\epsilon}_{total}^{VV} \equiv \bar{\epsilon}_{VV} + \mathcal{D}_{VG}$ and is therefore enhanced with respect to classical flows at uniform viscosity. This budget allows a complete expression of the mean energy dissipation rate $\bar{\epsilon}_{total}^{VV}$ to be written, viz. Talbot *et al.* (2013), Campbell & Turner (1985), $\bar{\epsilon}_{total}^{VV} \approx \frac{\nu_h}{\nu_l} v \left(\frac{\partial \overline{u_i}}{\partial x_j} \right)^2$.

The last part of the paper is dedicated to the scale-by-scale energy budget equation. Instantaneous Navier-Stokes equation, free from external forces, is first written for the **total** velocity, viz. $\frac{\partial u_i}{\partial t} + u_j \frac{\partial u_i}{\partial x_j} = -\frac{1}{\rho} \frac{\partial p}{\partial x_i} + \frac{\partial}{\partial x_j} [v \tau_{ij}]$, with $\tau_{ij} = \frac{\partial u_i}{\partial x_j} + \frac{\partial u_j}{\partial x_i}$. Two points of the flow, \vec{x}^+ and \vec{x}^- , separated by the increment \vec{r} such as $\vec{x}^+ = \vec{x}^- + \vec{r}$ are considered. Following the methodology suggested in Danaila

et al. (2004), Navier-Stokes equation for the total velocity with variable viscosity is written at these two points They are subtracted one from the other and further multiplied by twice the velocity increment Δu_i and averaged. All terms are similar to those present in the classical scale-by-scale energy budget equations, except the terms involving the viscosity which must include several contributions, similarly to the one-point energy budget. After numerous manipulations which are not detailed here, the scale-by-scale energy budget equation in VVF is finally given by

$$\begin{aligned}
& \bar{U}_j \frac{\partial}{\partial x_j} \overline{(\Delta u_i)^2} + \partial_{x_j} \overline{\frac{u_j^+ + u_j^-}{2} (\Delta u_i)^2} + \partial_{r_j} \overline{\Delta u_j (\Delta u_i)^2} + \overline{\Delta u_i \Delta u_j} \frac{\partial \bar{U}_i}{\partial x_j} \\
& = \\
& -\frac{2}{\rho} \partial_{x_i} \overline{\Delta p \Delta u_i} + \frac{\partial^2}{\partial r_j^2} (\overline{v^+ + v^-}) (\Delta u_i)^2 + \frac{1}{2} \overline{v^+ + v^-} \frac{\partial^2 (\overline{(\Delta u_i)^2}}{\partial x_j^2} \\
& - 2\bar{\epsilon}_{VV}^+ - 2\bar{\epsilon}_{VV}^- + \text{Viscosity terms}. \quad (2)
\end{aligned}$$

All terms are classical, except those formally denoted as 'Viscosity terms' which involve viscosity fluctuations and viscosity gradients at any scale \vec{r} , Eq. (3).

$$\begin{aligned}
& \text{Viscosity terms} = \\
& -\frac{\partial^2 (\overline{v^+ + v^-})}{\partial r_j^2} (\Delta u_i)^2 - \frac{\partial (\overline{v^+ + v^-})}{\partial r_j} \frac{\partial (\overline{(\Delta u_i)^2}}{\partial r_j} \\
& + (\overline{v^+ - v^-}) \frac{\partial}{\partial r_j} \frac{\partial}{\partial x_j} (\Delta u_i)^2 \\
& + \frac{\partial}{\partial x_j} (\overline{v^+ + v^-}) \left[\frac{\partial}{\partial x_j} (\overline{(\frac{\Delta u_i}{2})^2}) + \frac{\partial}{\partial x_i} (\overline{\Delta u_i \Delta u_j}) \right] \\
& + \frac{\partial}{\partial x_j} (\Delta v) \left[\frac{\partial}{\partial r_j} (\overline{(\frac{\Delta u_i}{2})^2}) + \frac{\partial}{\partial r_i} (\overline{\Delta u_i \Delta u_j}) \right] \\
& + \frac{\partial}{\partial r_j} (\Delta v) \left[\frac{\partial}{\partial x_j} (\overline{(\frac{\Delta u_i}{2})^2}) + \frac{\partial}{\partial x_i} (\overline{\Delta u_i \Delta u_j}) \right] \\
& + 2 \frac{\partial}{\partial r_j} (\overline{v^+ + v^-}) \left[\frac{\partial}{\partial x_j} (\overline{(\frac{\Delta u_i}{2})^2}) + \frac{\partial}{\partial x_i} (\overline{\Delta u_i \Delta u_j}) \right]. \quad (3)
\end{aligned}$$

This expression is consistent with the one-point kinetic energy budget, Eq. (1), in the limit of large scales. Thus, the balance between terms in VVF scale-by-scale energy budget equation is different from that in CVF. It will be argued that the importance of the advection term decreases in the near field, whereas the viscous terms are more and more important for increasing downstream locations.

It is worth noting that the "Viscosity terms", although they depend on viscosity, are present at large scales thus correcting the belief that the viscosity is reduced to a small-scale quantity. Whereas viscosity itself destroys kinetic energy, the viscosity gradients play a clear role of production of kinetic energy. Two flow regions may be distinguished: –the near field, where mixing between the two fluids occurs. In this region, it is reasonable to expect that the majority of terms in Eq. (2) is non-negligible.

–the far field, for which the central region of the flow is already mixed, although the viscosity of the flow continuously varies with the downstream location, say x_1 . Therefore, we consider in this region that $\bar{V}^+ \approx \bar{V}^-$ over scales \vec{r} ranging between the Kolmogorov and the integral scales (the latter being considered much smaller than the scale over which the decay takes place).

SIMILARITY AT ANY SCALE IN A VARIABLE VISCOSITY FLOW

In this last section, we address the question of the equilibrium self-similarity, as introduced by George & Gibson (1992) in the spectral space and Antonia *et al.* (2003) in real space. It is of interest to inquire into the similarity of all scales on the axis of a round jet, since Re_λ (the Reynolds number based on the Taylor's microscale) is expected to remain constant along the axis in the jet far field Tennekes & Lumley (1975).

Assuming

- local homogeneity and isotropy
- flow stationarity
- inhomogeneity along the jet axis (x_1) only
- lateral diffusion (no shear in the jet central region)
- \overline{U}_1 and \overline{v} only depend on x_1
- slight variations of $\overline{\epsilon}_{VV}$ over scales smaller than the integral scale *ie* $\overline{\epsilon}_{VV} = \overline{\epsilon}_{VV}^+$,

Eq. (2) in the central region of a round jet issuing into a more viscous fluid yields

$$\begin{aligned} \overline{U}_1 \frac{\partial}{\partial x_1} (\overline{\Delta u_i})^2 + \partial_{r_j} \overline{\Delta u_j} (\overline{\Delta u_i})^2 + 2 \frac{d\overline{U}_1}{dx_1} ((\Delta u_1)^2 - (\Delta u_2)^2) \\ + \frac{\partial}{\partial x_2} (\overline{u_2 + u_2^+}) (\overline{\Delta u_i})^2 \\ = \\ 2\overline{v} \frac{\partial^2}{\partial r_j^2} (\overline{\Delta u_i})^2 + \frac{d\overline{v}}{dx_1} \frac{\partial}{\partial x_1} (\overline{\Delta u_i})^2 - 2\overline{\epsilon}_{VV}. \end{aligned} \quad (4)$$

In the central region of the round jet all terms depend on r only, thus particular expressions for operators divergence and Laplacian can be chosen, namely in spherical coordinates. By following the classical approach Monin & Yaglom (1975), Danaïla *et al.* (2004), we finally obtain

$$\begin{aligned} -\overline{\Delta u_1} (\overline{\Delta u_i})^2 + 2\overline{v} \frac{d}{dr} (\overline{\Delta u_i})^2 \\ - \left(\overline{U}_1 + \frac{d\overline{v}}{dx_1} \right) \frac{1}{r^2} \int_0^r s^2 \frac{\partial (\overline{\Delta u_i})^2}{\partial x_1} ds \\ - 2 \frac{d\overline{U}_1}{dx_1} \frac{1}{r^2} \int_0^r s^2 \left((\overline{\Delta u_1})^2 - (\overline{\Delta u_2})^2 \right) ds \\ - \frac{1}{r^2} \int_0^r s^2 \left[\frac{\partial}{\partial x_2} (\overline{u_2 + u_2^+}) (\overline{\Delta u_i})^2 \right] ds = \frac{4}{3} \overline{\epsilon}_{VV} r, \end{aligned} \quad (5)$$

where s is a dummy variable. Whether or not the turbulent diffusion is present along the axis of a round jet, is still controversial, even for constant viscosity flows, Hussein *et al.* (1994).

In order to examine the conditions under which Eq. (5) satisfies similarity, we need to assume functional forms for the terms in this equation. Following Antonia *et al.* (2003) and Burattini *et al.* (2005), we take

$$\begin{aligned} \overline{(\Delta u_i)^2} &= Q(x_1) f(\xi) \\ \overline{(\Delta u_1)^2} &= M(x_1) e(\xi) \\ \overline{(\Delta u_2)^2} &= R(x_1) h(\xi) \\ -\overline{\Delta u_1} (\overline{\Delta u_i})^2 &= T(x_1) g(\xi), \end{aligned} \quad (6)$$

where $\xi = r/\mathcal{L}$ and \mathcal{L} is a characteristic length scale, to be determined. A possible dependence on the initial conditions is not explicitly considered here. The other terms may be written in a similar fashion, but we focus here only

on some of them. $Q(x_1)$ and $T(x_1)$ are scales that characterize the second-order and the third-order structure functions, respectively. The lower-case functions represent the shape of the involved structure functions. The separation between functions of x_1 and ξ allows solutions of the transport equation for which a relative balance among all of the terms is maintained as the flow progresses downstream to be obtained. Upon substituting Eqs. (6) into Eq. (5), we obtain (after differentiating and rearranging)

$$\begin{aligned} T(x_1) g(\xi) + 2\overline{v} Q(x_1) \frac{1}{\mathcal{L}} f'(\xi) \\ - \frac{\overline{U}_1 Q'(x_1)}{r^2} \mathcal{L}^3 \Gamma_1 - \frac{d\overline{v}}{dx_1} \frac{Q'(x_1)}{r^2} \mathcal{L}^3 \Gamma_1 \\ + \frac{\overline{U}_1 Q(x_1)}{r^2} \frac{d\mathcal{L}}{dx_1} \mathcal{L}^2 \Gamma_2 \\ + \frac{d\overline{v}}{dx_1} \frac{Q(x_1)}{r^2} \frac{d\mathcal{L}}{dx_1} \mathcal{L}^2 \Gamma_2 - 2 \frac{d\overline{U}_1}{dx_1} \frac{M(x_1)}{r^2} \mathcal{L}^3 \Gamma_3 \\ + 2 \frac{d\overline{U}_1}{dx_1} \frac{R(x_1)}{r^2} \mathcal{L}^3 \Gamma_4 = \frac{4}{3} (\overline{\epsilon})_{hom} r. \end{aligned} \quad (7)$$

where $\Gamma_1 = \int_0^{r/\mathcal{L}} \frac{s^2}{\mathcal{L}^2} f(\xi) d(\frac{s}{\mathcal{L}})$; $\Gamma_2 = \int_0^{r/\mathcal{L}} \frac{s^3}{\mathcal{L}^3} f'(\xi) d(\frac{s}{\mathcal{L}})$; $\Gamma_3 = \int_0^{r/\mathcal{L}} \frac{s^2}{\mathcal{L}^2} e(\xi) d(\frac{s}{\mathcal{L}})$; $\Gamma_4 = \int_0^{r/\mathcal{L}} \frac{s^2}{\mathcal{L}^2} h(\xi) d(\frac{s}{\mathcal{L}})$. Note that the following relation has been used $\frac{\partial \xi}{\partial x_1} = -r \mathcal{L}^{-2} \frac{d\mathcal{L}}{dx_1}$. After some rearranging and requiring that, for equilibrium similarity, all terms function of x_1 must evolve in the streamwise direction in the same way, we obtain

$$\frac{T(x_1) \mathcal{L}}{\overline{v}(x_1) Q(x_1)} = const. \quad (8)$$

$$\frac{\overline{U}_1 Q'(x_1) \mathcal{L}^2}{\overline{v}(x_1) Q(x_1)} = const. \quad (9)$$

$$\frac{d\overline{v}(x_1)}{dx_1} \frac{Q' \mathcal{L}^2}{\overline{v} Q(x_1)} = const. \quad (10)$$

$$\frac{\overline{U}_1}{\overline{v}(x_1)} \frac{d\mathcal{L}}{dx_1} \mathcal{L} = const. \quad (11)$$

$$\frac{\overline{\epsilon}_{VV}}{\overline{v}(x_1)} \frac{\mathcal{L}^2}{Q(x_1)} = const. \quad (12)$$

The other terms may be written similarly, but the information they provide is redundant with respect to what follows. Supposing that a similarity variable for $Q(x_1)$ is the total kinetic energy, *i.e.* $Q(x_1) \sim u_t^2$, then from Eq.(12), a characteristic scale can be identified with the Taylor microscale $\lambda \equiv \sqrt{\frac{Q\overline{v}}{\overline{\epsilon}_{VV}}}$, therefore $\mathcal{L} \equiv \lambda$. We consider the following power laws for \overline{U}_1 as well as for u' , the root mean square of the total kinetic energy u_t^2 ,

$$\overline{U}_1 \sim x_1^{-n_u}, \quad u' \sim x_1^{-n_u}, \quad \overline{v} \sim x_1^{n_v}, \quad (13)$$

with $n_U > 0$, $n_u > 0$, $n_v > 0$. Injecting (13) into Eq. (11), it can be inferred that

$$\mathcal{L} \sim x_1^{\frac{n_U+n_v+1}{2}}. \quad (14)$$

Combining Eq.8 to Eq.13 and assuming that $T(x_1)/Q(x_1) \sim u'$, we deduce the following relations between the power law exponents

$$n_U = n_u, \quad (15)$$

and

$$n_v = 1 - n_U. \quad (16)$$

Equation (15) simply signifies that the decaying laws for the streamwise mean velocity and the associated fluctuation root mean square are similar. This result fully supports the hypothesis of self-similarity.

This very simple relation reflects the fact that $Re_{\mathcal{L}}$ (or, Re_{λ} as the characteristic scale has been identified with the Taylor microscale), is constant along the axis of the jet. Hereafter, (at least) three scenarii are possible. The first one is that when as in classical round jets, both the streamwise velocity and the fluctuations root mean squared u' decay as x_1^{-1} , as shown by Talbot *et al.* (2009). These values are fully consistent with the conservation of the jet momentum, Tennekes & Lumley (1975). Then, Eq. (16) ineluctably leads to $n_v = 0$, which is to say that the jet evolves and entrains ambient fluid with the same viscosity. Therefore, our analysis is fully compatible with the constant-viscosity jets for which Re_{λ} is conserved. The second possibility is that corresponding to real jets evolving in a variable-viscosity host fluid, for which $n_v \neq 0$. Therefore, if Eq. (16) holds, then $n_U \neq 1$ and this signifies that the classical conservation of the jet momentum is not respected, Hussain & Zedan (1978). Then, Re_{λ} might be conserved along the axis of the variable-viscosity jet, but then the jet momentum is not conserved. The last possibility is for $n_v \neq 0$, Eq. (16) does not hold, so Re_{λ} is not conserved. All these possibilities are complex, and deserve further experimental and numerical investigations.

CONCLUSION

With respect to the classical constant-viscosity jet, the variable-viscosity jet of a fluid issuing into a more viscous ambient, exhibits:

–in the very near field, enhanced entrainment, important turbulent fluctuations.

–in the far field, turbulent fluctuations are destroyed by the increased ambient viscosity and R_{λ} might not remain constant. The general message of this contribution is that whereas the viscosity itself indeed acts at the level of smallest scales, flows with viscosity variations at a large scale (such as jets issuing in different environment) are characterised by effects of viscosity variations at any scale, including the largest. A simple visualisation of the scalar dispersion allows us to observe a significant disparity between

VVF and CVF behaviours, leading us to say that the viscosity affects the topology and the dynamics of the whole flow at all scales.

REFERENCES

- Amiellh, M., Djeridane, T., Anselmet, F. & Fulachier, L. 1996 Velocity near-field of variable density turbulent jets. *International Journal of Heat and mass transfer* **39**, 2149–2164.
- Antonia, R. A., Smalley, R. J., Zhou, T., Anselmet, F. & Danaïla, L. 2003 Similarity of energy structure functions in decaying homogeneous isotropic turbulence. *Journal of Fluid Mechanics* **487**, 245–269.
- Burattini, P., Antonia, R. A. & Danaïla, L. 2005 Similarity in the far field of a turbulent round jet. *Physics of fluids* **17**, 025101–.
- Campbell, I. H. & Turner, J. S. 1985 Turbulent mixing between fluids with different viscosities. *Letters to Nature* **313**, 39–42.
- Campbell, I. H. & Turner, J. S. 1986 The influence of viscosity on fountains in magma chamber. *Journal of Petrology* **27**, 1–30.
- Danaïla, L., Antonia, R A & Burattini, P. 2004 Progress in studying small-scale turbulence using 'exact' two-point equations. *New Journal of Physics* **6**, 128.
- George, W.K. & Gibson, M. M. 1992 The self-preservation of homogeneous shear flow turbulence. *Exp. in Fluids* **13**, 229–1509.
- Hussain, A. K. M. F. & Zedan, M. F. 1978 Effects of the initial condition on the axisymmetric free shear layer. *Phys. of Fluids* **21(7)**, 1100–1112.
- Hussein, H.J., Capp, S. P. & George, William K. 1994 Velocity measurements in a high-reynolds-number, momentum-conserving, axisymmetric, turbulent jet. *Journal of Fluid Mechanics* **258**, 31–75.
- Lee, K., Girimaji, S. & Kerimo, J. 2008 Validity of Taylor's dissipation-viscosity independence postulate in variable-viscosity turbulent fluid mixtures. *Phys. Rev. Lett.* **101** (7), 074501–.
- Monin, A.S. & Yaglom, A.M. 1975 *Statistical Fluid Mechanics*. MIT Press, Cambridge, MA.
- Pitts, W. M. 1991 Effects of global density ratio on the centerline mixing behavior of axisymmetric turbulent jets. *Experiments in Fluids* **11**, 125–134.
- Taguelmimt, N., Danaïla, L. & Hadjadj, A. 2014 Effects of viscosity variations in temporal mixing layer. *J. Phys.: Conf. Ser.* **530**, 012057.
- Talbot, B. 2009 *Mélange et dynamique de la turbulence en écoulements libres à viscosité variable*. PhD thesis, INSA de Rouen.
- Talbot, B., Danaïla, L. & Renou, B. 2013 Variable-viscosity mixing in the very near field of a round jet. *Physica Scripta* **T155**, 014006.
- Talbot, B., Mazellier, N., Renou, B., Danaïla, L. & Boukhalfa, M. 2009 Time-resolved velocity and concentration measurements in variable-viscosity turbulent jet flow. *Experiments in Fluids* **47**, 769–787.
- Tennekes, I. & Lumley, J. 1975 *A first course in turbulence*. MIT Press, Cambridge, MA.